 CMC, vol.19, no.1, pp.17-36, 2010

A Backward Group Preserving Scheme for Multi-Dimensional Backward Wave Problems

Chih-Wen Chang[1,2] **and Chein-Shan Liu**[3]

Abstract: The present study shows a backward group preserving scheme (BGPS) to deal with the multi-dimensional backward wave problem (BWP). The BWP is well-known as seriously ill-posed because the solution does not continuously count on the given data. When three numerical experiments are tested, we reveal that the BGPS is applicable to the multi-dimensional BWP. Even with noisy final data, the BGPS is also robust against perturbation. The numerical results are very pivotal in the computations of multi-dimensional BWP.

Keywords: Wave equation, Backward wave problem, Strongly ill-posed problem, Backward group preserving scheme (BGPS), Group preserving scheme (GPS)

1 Introduction

Wave problems that appear from engineering applications are usually divided into forward wave problems and backward wave problems. There are many approaches for dealing with forward wave problems, for example, the method of fundamental solution [Gu, Young and Fan (2009)], the time-marching method of fundamental solutions [Young, Gu and Fan (2009)], the analytical fundamental solution [Czygan and Estorff (2003)], the wave finite element solution [Zhou and Ichchou (2010)], the energy preserving schemes [Chabassier and Joly (2010)], and the shooting methods [Yang (2006)].

For the backward wave problems (BWPs), Lesnic (2002) has proposed the Adomain decomposition method to tackle the BWP. He pointed out that for the forward problem the convergence of the Adomain decomposition method is faster than that for the backward problem. Moreover, the BWP as mentioned by Ames and Straugham (1997) has pivotal applications in optimal control theory and geo-

[1] Grid Applied Technology Division, National Center for High-Performance Computing, Taichung 40763, Taiwan
[2] Corresponding author, Tel.: +886-4-24620202x860. E-mail address: d9351002@nchc.org.tw
[3] Department of Civil Engineering, National Taiwan University, Taipei 10617, Taiwan

physics. Recently, Liu (2010) has employed the separating characteristic property of kernel function and eigenfunctions expansion techniques to derive a semi-analytical solution of BWP and obtained good results.

In this paper, we propose the backward group preserving scheme (BGPS) to deal with the BWPs. This approach was first employed by Liu, Chang and Chang (2006) to solve the homogeneous BHCP. Lack of need for a priori regularization in use, makes the BGPS more appealing for inverse problems with a final value problem. In fact, the BGPS was an extension of the work by Liu (2004) by taking time regression of equations into account in the formation of backward group theory. After that, Liu (2006) and Liu, Chang and Chang (2010) extended the BGPS to solve the backward in time Burgers equation and the backward in time advection-dispersion equation, respectively. The current method would provide us a more succinct numerical procedure than other approaches to copy with the BWP.

The present paper is organized as follows. Section 2 illustrates the multi-dimensional homogeneous BWP and its final condition, boundary conditions and semi-discretization. We give a sketch of the group preserving scheme (GPS) [Liu (2001)] for ordinary differential equations (ODEs) and derive the BGPS for the backward differential equations system in Section 3. In Section 4, we use the semi-discretization and the BGPS to solve some numerical experiments. Finally, some concluding remarks are given in Section 5.

2 Backward wave problems

The multi-dimensional homogeneous BWP we ponder is respectively given by the following equations:

$$\frac{\partial^2 u}{\partial t^2} = c^2 \Delta u \text{ in } \Omega, \tag{1}$$

$$u = u_{\mathrm{B}} \text{ on } \Gamma_{\mathrm{B}}, \tag{2}$$

$$u = u_{\mathrm{F}} \text{ on } \Gamma_{\mathrm{F}}, \tag{3}$$

where u is the displacement of a rectangular volume and c is the velocity of a propagation wave. We take a bounded domain D in R^j, $j = 1, 2, 3$ and a spacetime domain $\Omega = D \times (0,T)$ in R^{j+1} for a final time $T > 0$, and write two surfaces $\Gamma_{\mathrm{B}} = \partial D \times [0,T]$ and $\Gamma_{\mathrm{F}} = \partial D \times \{T\}$ of the boundary $\partial\Omega$. Δ represents the j-dimensional Laplacian operator. While Eqs. (1)-(3) constitute a j-dimensional backward wave problem for a given boundary data u_B: $\Gamma_{\mathrm{B}} \mapsto R$ and a final data u_{F}: $\Gamma_{\mathrm{F}} \mapsto R$. For the existence and uniqueness of solution of BWP, Bourgin and Duffin (1939), and Abdul-Latif and Diaz (1971) have given a geometric proof of the

uniqueness of the one-dimensional wave equation under the Dirichlet conditions. Fox and Pucci (1958) have addressed the existence issue of this problem in detail. Levine and Vessella (1985) have concerned about the existence and continuous on data and treated the problem in Hilbert space.

Applying a semi-discrete procedure to Eq. (1), yields a coupled system of ODEs:

$$\dot{u}_{i,j,k}(t) = v_{i,j,k}(t)$$

$$\dot{v}_{i,j,k}(t) = -c^2 \left\{ \frac{[u_{i+1,j,k}(t) - 2u_{i,j,k}(t) + u_{i-1,j,k}(t)]}{(\Delta x)^2} + \frac{[u_{i,j+1,k}(t) - 2u_{i,j,k}(t) + u_{i,j-1,k}(t)]}{(\Delta y)^2} + \frac{[u_{i,j,k+1}(t) - 2u_{i,j,k}(t) + u_{i,j,k-1}(t)]}{(\Delta z)^2} \right\}, \quad (4)$$

where $\Delta x, \Delta y$ and Δz are uniform spatial lengths in x, y and z directions, $u_{i,j,k}(t) = u(i\Delta x, j\Delta y, k\Delta z, t), v_{i,j,k}(t) = v(i\Delta x, j\Delta y, k\Delta z, t), \dot{u}$ denotes the differential of u with respect to t, and $\dot{v}$ denotes the differential of v with respect to t. Obviously, in Eq. (4) there are totally $2n^3$ coupled linear differential equations for the n^3 variables $u_{i,j,k}(t)$, $i,j,k = 1,2,\cdots,n$, and these n^3 variables $v_{i,j,k}(t)$, $i,j,k = 1,2,\cdots,n$, which, even for a specified final time condition can be numerically integrated by the BGPS developed in Section 3.2 for the resulting backward ODEs.

3 Numerical methods

We will divide problems and solvers into two classes: 3.1 Forward problems and group preserving scheme, and 3.2 Backward problems and backward group preserving scheme.

3.1 Forward problems and Group preserving scheme

3.1.1 Dynamics on a future cone

GPS can preserve the internal symmetry group of the considered system. For nonlinear differential equations systems, Liu (2001) has embedded them into the augmented dynamical systems, which concern with not only the evolution of state variables but also the evolution of the magnitude of state variables vector. That is, for an n ordinary differential equations system:

$$\dot{\mathbf{x}} = \mathbf{f}(\mathbf{x}, t), \ \mathbf{x} \in \mathbb{R}^n, \ t \in \mathbb{R}^+, \quad (5)$$

we can embed it into the following n+1-dimensional augmented dynamical system:

$$\frac{d}{dt}\begin{bmatrix}\mathbf{x}\\ \|\mathbf{x}\|\end{bmatrix}=\begin{bmatrix}\mathbf{0}_{n\times n} & \frac{\mathbf{f}(\mathbf{x},t)}{\|\mathbf{x}\|}\\ \frac{\mathbf{f}^{\mathrm{T}}(\mathbf{x},t)}{\|\mathbf{x}\|} & 0\end{bmatrix}\begin{bmatrix}\mathbf{x}\\ \|\mathbf{x}\|\end{bmatrix}. \tag{6}$$

Here, we assume $\|\mathbf{x}\|>0$ and hence, the above system is well-defined.

It is obvious that the first row in Eq. (6) is the same as the original Eq. (5), but the inclusion of the second row in Eq. (6) gives us a Minkowskian structure of the augmented state variables of $\mathbf{X}:=(\mathbf{x}^{\mathrm{T}},\|\mathbf{x}\|)^{\mathrm{T}}$ satisfying a future cone condition as shown in Fig. 1:

$$\mathbf{X}^{\mathrm{T}}\mathbf{g}\mathbf{X}=0, \tag{7}$$

where

$$\mathbf{g}=\begin{bmatrix}\mathbf{I}_n & \mathbf{0}_{n\times 1}\\ \mathbf{0}_{1\times n} & -1\end{bmatrix} \tag{8}$$

is a Minkowski metric. $\mathbf{I}_n$ is the identity matrix of order n, and the superscript T denotes the transpose. In terms of $(\mathbf{x}^{\mathrm{T}},\|\mathbf{x}\|)$, Eq. (7) holds, as

$$\mathbf{X}^{\mathrm{T}}\mathbf{g}\mathbf{X}=\mathbf{x}\cdot\mathbf{x}-\|\mathbf{x}\|^2=\|\mathbf{x}\|^2-\|\mathbf{x}\|^2=0, \tag{9}$$

where the dot between two n-dimensional vectors represents their Euclidean inner product. The cone condition is thus the most natural constraint that we can impose on the dynamical system (6).

Consequently, we have an n+1-dimensional augmented system:

$$\dot{\mathbf{X}}=\mathbf{A}\mathbf{X} \tag{10}$$

with a constraint (7), where

$$\mathbf{A}:=\begin{bmatrix}\mathbf{0}_{n\times n} & \frac{\mathbf{f}(\mathbf{x},t)}{\|\mathbf{x}\|}\\ \frac{\mathbf{f}^{\mathrm{T}}(\mathbf{x},t)}{\|\mathbf{x}\|} & 0\end{bmatrix} \tag{11}$$

is an element of the Lie algebra $so(n,1)$ of the proper orthochronous Lorentz group $SO_o(n,1)$, satisfying

$$\mathbf{A}^{\mathrm{T}}\mathbf{g}+\mathbf{g}\mathbf{A}=0. \tag{12}$$

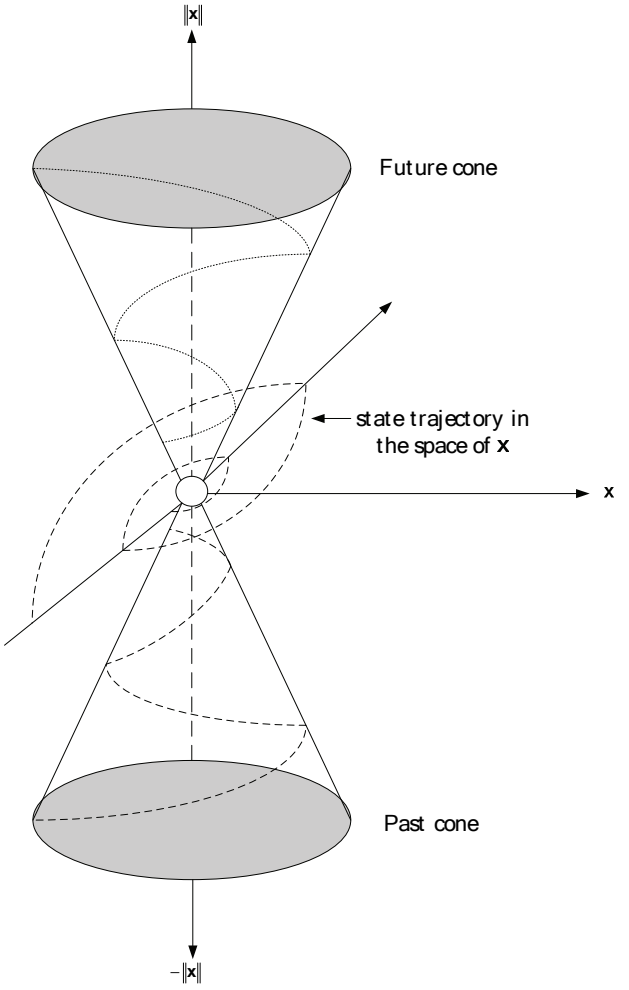

Figure 1: The construction of deleted cones in the Minkowski space for forward and backward problems signifies a conceptual breakthrough. The trajectory observed in the state space $\mathbf{x}$ is a parallel projection of the trajectory in the null cones along the $\|\mathbf{x}\|$ or $-\|\mathbf{x}\|$-axis.

This fact prompts us to employ the group preserving scheme, and its discretized mapping $\mathbf{G}$ exactly preserves the following properties:

$$\mathbf{G}^{\mathrm{T}}\mathbf{g}\mathbf{G} = \mathbf{g}, \tag{13}$$

$$\det\mathbf{G} = 1, \tag{14}$$

$$G_0^0 > 0, \tag{15}$$

where G_0^0 is the 00th component of $\mathbf{G}$. Such $\mathbf{G}$ is an element of $SO_o(n,1)$. The term orthochronous should be understood as the preservation of the sign of $\|\mathbf{x}\| > 0$. The discretization procedure will be presented depending on each problem after this section.

Remarkably, the original n-dimensional dynamical system (5) in the usual Euclidean space E^n can be embedded very naturally into an augmented n+1-dimensional dynamical system (10) in the Minkowski space M^{n+1} and these two systems are mathematically equivalent. Although the dimension of the new system rises by one, Liu (2001) has shown that, under the Lipschitz condition of

$$\|\mathbf{f}(\mathbf{x},t) - \mathbf{f}(\mathbf{y},t)\| \leq L\|\mathbf{x}-\mathbf{y}\|, \ \forall(\mathbf{x},t),(\mathbf{y},t) \in \mathbf{D}, \tag{16}$$

where $\mathbf{D}$ is a domain in $R^n \times R^+$, and L is known as a Lipschitz constant, the new system has the advantage of admitting a group preserving numerical scheme as follows:

$$\mathbf{X}_{\ell+1} = \mathbf{G}(\ell)\mathbf{X}_\ell, \tag{17}$$

where $\mathbf{X}_\ell$ stands for the numerical evaluation of $\mathbf{X}$ at the discrete time t_ℓ, and $\mathbf{G}(\ell) \in SO_o(n,1)$ is the group evaluation at time t_ℓ.

3.1.2 GPS for forward differential equations system

To give a step by step numerical scheme, we suppose that $\mathbf{A}(\ell)$ in Eq. (10) is a constant matrix, taking its value at the $\ell - th$ step. An exponential mapping of $\mathbf{A}(\ell)$ for the interval $t_\ell \leq t < t_\ell + \Delta t$, when the time parameter t in Eq. (11) is approximately fixed as $t = t_\ell$ admits:

$$\exp[\Delta t\mathbf{A}(\ell)] = \begin{bmatrix} \mathbf{I}_n + \frac{(a_\ell - 1)}{\|\mathbf{f}_l\|^2}\mathbf{f}_\ell\mathbf{f}_\ell^{\mathrm{T}} & \frac{b_\ell \mathbf{f}_\ell}{\|\mathbf{f}_\ell\|} \\ \frac{b_\ell \mathbf{f}_\ell^{\mathrm{T}}}{\|\mathbf{f}_\ell\|} & a_\ell \end{bmatrix}, \tag{18}$$

where

$$a_\ell := \cosh\left(\frac{\Delta t\,\|f_\ell\|}{\|x_\ell\|}\right), \ b_\ell := \sinh\left(\frac{\Delta t\,\|f_\ell\|}{\|x_\ell\|}\right). \tag{19}$$

For saving notation, we use $\mathbf{f}_\ell = \mathbf{f}(\mathbf{x}_\ell, t_\ell)$. Substituting the above $exp[\Delta t\mathbf{A}(\ell)]$ for $\mathbf{G}(\ell)$ into Eq. (17) and taking its first row, we obtain

$$\mathbf{x}_{\ell+1} = \mathbf{x}_\ell + \frac{(a_\ell - 1)\mathbf{f}_\ell \cdot \mathbf{x}_\ell + b_\ell\|\mathbf{x}_\ell\| \ \|\mathbf{f}_\ell\|}{\|\mathbf{f}_\ell\|^2}\mathbf{f}_\ell = \mathbf{x}_\ell + \eta_\ell \mathbf{f}_\ell. \tag{20}$$

From $\mathbf{f}_\ell \cdot \mathbf{x}_\ell \geq -\|\mathbf{f}_\ell\| \ \|\mathbf{x}_\ell\|$, we can prove that

$$\eta_\ell \geq \left[1-\exp\left(-\frac{\Delta t\,\|\mathbf{f}_\ell\|}{\|\mathbf{x}_\ell\|}\right)\right]\frac{\|\mathbf{x}_\ell\|}{\|\mathbf{f}_\ell\|} > 0,\ \forall \Delta t > 0. \tag{21}$$

This scheme is group properties preserved for all $\Delta t > 0$.

3.2 Backward problems and backward group preserving scheme

3.2.1 Dynamics on a past cone

Corresponding to the initial value problems governed by Eq. (5) with a specified initial value $\mathbf{x}(0)$ at an initial time, for many systems in the engineering applications, the final value problems may happen because one wants to retrieve the past histories of state variables exhibited in the physical models. These time backward problems of ordinary differential equations type can be described by

$$\dot{\mathbf{x}} = \mathbf{f}(\mathbf{x},t),\ \mathbf{x} \in \mathbb{R}^n,\ t \in \mathbb{R}^-. \tag{22}$$

With a specified final value $\mathbf{x}(0)$ at $t = 0$, we intend to recover the past values of $\mathbf{x}$ in the past time of $t < 0$.

We can embed Eq. (22) into the following n+1-dimensional augmented dynamical system:

$$\frac{d}{dt}\begin{bmatrix}\mathbf{x}\\ -\|\mathbf{x}\|\end{bmatrix} = \begin{bmatrix}\mathbf{0}_{n\times n} & -\frac{\mathbf{f}(\mathbf{x},t)}{\|\mathbf{x}\|}\\ -\frac{\mathbf{f}^{\mathrm{T}}(\mathbf{x},t)}{\|\mathbf{x}\|} & 0\end{bmatrix}\begin{bmatrix}\mathbf{x}\\ -\|\mathbf{x}\|\end{bmatrix}. \tag{23}$$

It is obvious that the first row in Eq. (23) is the same as the original Eq. (22), but the inclusion of the second row in Eq. (6) gives us a Minkowskian structure of the augmented state variables of $\mathbf{X} := (\mathbf{x}^{\mathrm{T}}, -\|\mathbf{x}\|)^{\mathrm{T}}$ satisfying a past cone condition:

$$\mathbf{X}^{\mathrm{T}}\mathbf{g}\mathbf{X} = \mathbf{x}\cdot\mathbf{x} - \|\mathbf{x}\|^2 = \|\mathbf{x}\|^2 - \|\mathbf{x}\|^2 = 0. \tag{24}$$

Here, we should stress that the cone condition imposed on the dynamical system (6) is a future cone as shown in Fig. 1, while that for the dynamical system (23) the cone condition (24) imposed is a past cone as shown in Fig. 1.

Consequently, we have an n+1-dimensional augmented system:

$$\dot{\mathbf{X}} = \mathbf{B}\mathbf{X} \tag{25}$$

with a constraint (24), where

$$\mathbf{B} := \begin{bmatrix}\mathbf{0}_{n\times n} & -\frac{\mathbf{f}(\mathbf{x},t)}{\|\mathbf{x}\|}\\ -\frac{\mathbf{f}^{\mathrm{T}}(\mathbf{x},t)}{\|\mathbf{x}\|} & 0\end{bmatrix}, \tag{26}$$

satisfying

$$\mathbf{B}^{\mathrm{T}}\mathbf{g}+\mathbf{g}\mathbf{B}=0, \tag{27}$$

which is a Lie algebra $so(n,1)$ of the proper orthochronous Lorentz group $SO_o(n,1)$. The term orthochronous used here is referred to the preservation of the sign of $-\|\mathbf{x}\|<0$.

According to the above Lie algebra property of $\mathbf{B}$, we can derive a backward group preserving scheme as Eq. (17) for Eq. (10):

$$\mathbf{X}_{\ell-1}=\mathbf{G}(\ell)\mathbf{X}_{\ell}. \tag{28}$$

The above is a backward single-step numerical scheme. Below we derive a group preserving scheme for Eq. (25).

3.2.2 BGPS for backward differential equations system

Similarly, by assuming that $\mathbf{B}(\ell)$ is a constant matrix, an exponential mapping of $\mathbf{B}(\ell)$ admits a closed-form representation:

$$\exp[-\Delta t\mathbf{B}(\ell)]=\begin{bmatrix}\mathbf{I}_n+\frac{(a_\ell-1)}{\|\mathbf{f}_\ell\|^2}\mathbf{f}_\ell\mathbf{f}_\ell^{\mathrm{T}} & \frac{b_\ell\mathbf{f}_\ell}{\|\mathbf{f}_\ell\|}\\ \frac{b_\ell\mathbf{f}_\ell^{\mathrm{T}}}{\|\mathbf{f}_\ell\|} & a_\ell\end{bmatrix}, \tag{29}$$

where a_ℓ and b_ℓ are still defined by Eq. (19).

Substituting the above $\exp[-\Delta t\mathbf{B}(\ell)]$ for $\mathbf{G}(\ell)$ into Eq. (28) and taking its first row, we obtain

$$\mathbf{x}_{\ell-1}=\mathbf{x}_\ell+\frac{(a_\ell-1)\mathbf{f}_\ell\cdot\mathbf{x}_\ell-b_\ell\|\mathbf{x}_\ell\|\ \|\mathbf{f}_\ell\|}{\|\mathbf{f}_\ell\|^2}\mathbf{f}_\ell=\mathbf{x}_\ell+\eta_\ell\mathbf{f}_\ell. \tag{30}$$

From $\mathbf{f}_\ell\cdot\mathbf{x}_\ell\le\|\mathbf{f}_\ell\|\ \|\mathbf{x}_\ell\|$, we can prove that

$$\eta_\ell\le\left[\exp\left(-\frac{\Delta t\,\|\mathbf{f}_\ell\|}{\|\mathbf{x}_\ell\|}\right)-1\right]\frac{\|\mathbf{x}_\ell\|}{\|\mathbf{f}_\ell\|}<0,\ \forall\Delta t>0. \tag{31}$$

This scheme is group properties preserved for all $\Delta t>0$.

Comparing Eqs. (30) with (20), we note that they have the same form except that the sign before $b_\ell\|\mathbf{x}_\ell\|\ \|\mathbf{f}_\ell\|$ in the numerators. We will call this numerical scheme a backward group preserving scheme (BGPS), which is slightly different from the group preserving scheme (GPS) introduced in Section 3.2.1 for the forward differential dynamics.

4 Numerical examples

We will apply the BGPS to the calculations of BWP through numerical examples. We are interested in the stability of our scheme when the input final measured data are contaminated by random noise for different problems. We can evaluate the stability by increasing the different levels of random noise in the final data:

$$\hat{\mathbf{u}}_{\mathrm{F}} = \mathbf{u}_{\mathrm{F}} + s[2R(i) - 1], \tag{32}$$

where $\mathbf{u}_{\mathrm{F}}$ is the final exact data, respectively. We use the function RANDOM_NUMBER given in Fortran to generate the noisy data $R(i)$, which are random numbers in [-1, 1], and s means the level of absolute noise. Then, the final noisy data $\hat{\mathbf{u}}_{\mathrm{F}}$ are used in the calculations. Usually, when the exact data is small, we employ the relative random noise to depict noise

$$s_r = \frac{s}{|\mathbf{u}_{\mathrm{F}}^{max}|} \times 100\%, \tag{33}$$

where $\mathbf{u}_{\mathrm{F}}^{max}$ is the maximum exact data.

4.1 Example 1

Consider the following one-dimensional BWP:

$$u_{tt} = u_{xx},\ 0 < x < \pi,\ 0 < t < T, \tag{34}$$

with the boundary conditions

$$u(0,t) = u(\pi,t) = 0, \tag{35}$$

and the final condition

$$u(x,T) = sin(T)sin(x),\ u_t(x,T) = cos(T)sin(x). \tag{36}$$

The data to be recovered are given by

$$u(x,t) = sin(t)sin(x),\ 0 \le t < T. \tag{37}$$

Note that the above BWP has a unique solution if and only if the ratio π/T is an irrational number. For this computational experiment, we used a time increment Δt = 0.001, a grid length $\Delta x = \pi/60$, c = 1, T = 1.5, and calculated this example by the BGPS. The accuracy as can be seen from Fig. 2 is rather good. Lesnic (2002) have

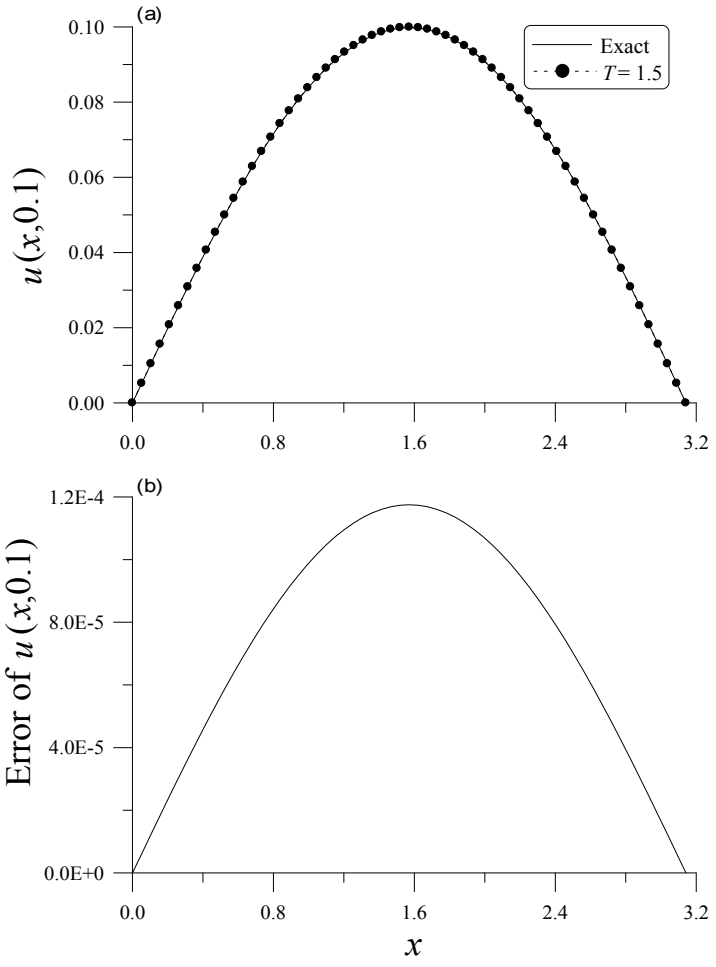

Figure 2: Comparisons of the exact solutions and numerical solutions with final time $T = 1.5$, and the corresponding numerical errors.

calculated this example by the Adomain decomposition method and shown that the solution is convergent very slowly with terminal times $T = 0.5$, 1 as shown in their Figure 4.

In this example, when the input final measured data are disturbed by the random noise, we are interested in the stability of BGPS, which is investigated by adding the level of random noise on the final data. The results of $T = 1.5$ are compared with the numerical result without considering the relative random noise in Fig. 3. Note that the relative noise level with $s_r = 10\%$ disturbs the numerical solutions a

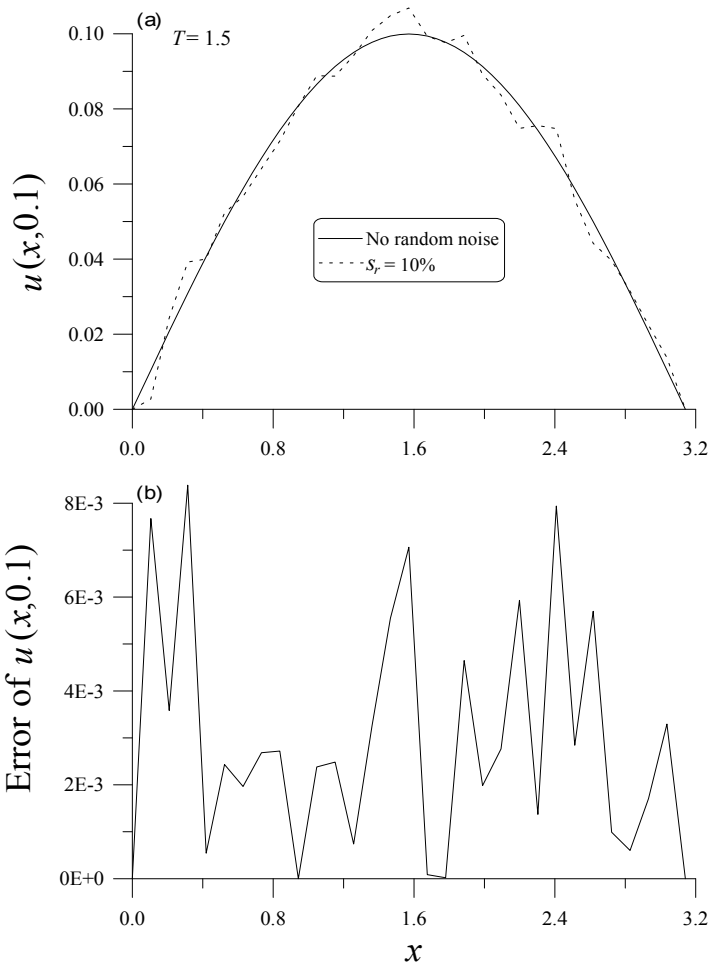

Figure 3: Comparisons of numerical solutions were made in (a) with different levels of noise $s_r = 0$, 10%, and (b) the corresponding numerical errors.

little from that without adding the noise.

4.2 Example 2

Let us further consider the two-dimensional BWP:

$$u_{tt} = 2(u_{xx} + u_{yy}),\ 0 < x < \pi,\ 0 < y < \pi,\ 0 < t < T, \tag{38}$$

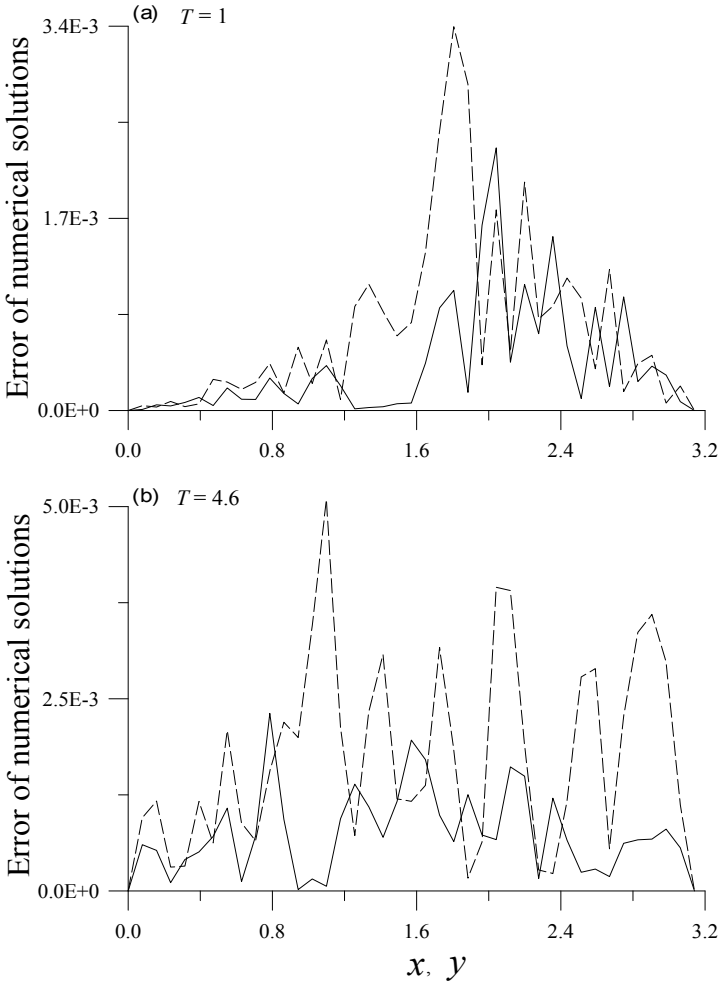

Figure 4: The errors of BGPS solutions for Example 2 are plotted in (a) with T = 1, and in (b) with T = 4.6.

with the boundary conditions

$$\begin{aligned} &u(0,y,t) = y,\ u(\pi,y,t) = \pi + y, \\ &u(x,0,t) = x,\ u(x,\pi,t) = \pi + x, \end{aligned} \tag{39}$$

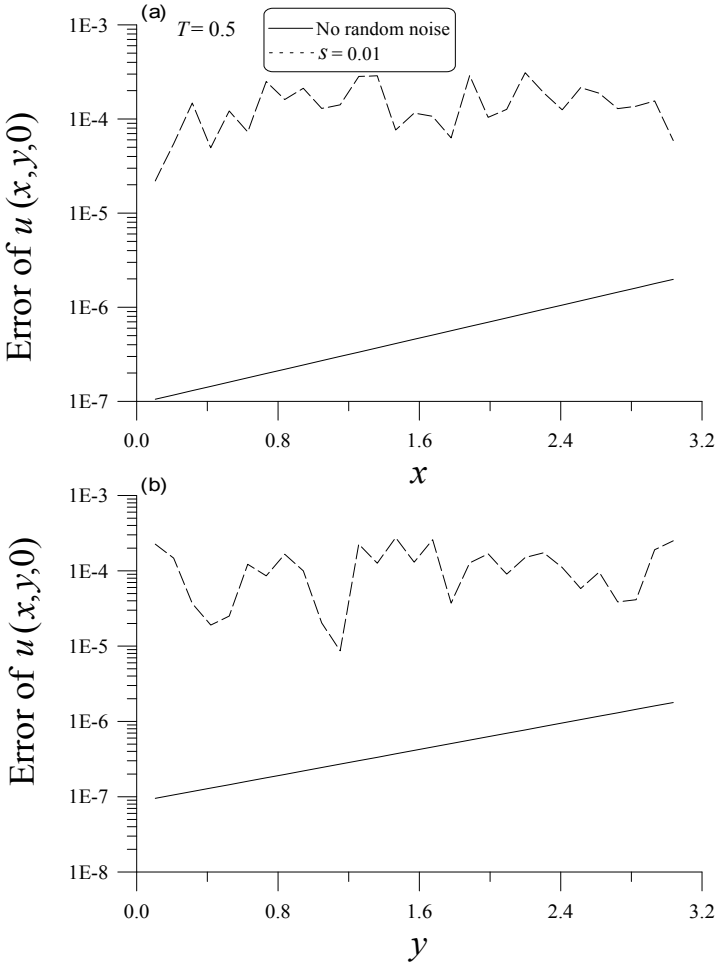

Figure 5: The numerical errors of BGPS solutions with and without random noise effect for Example 2 are plotted in (a) with respect to x at fixed $y = \pi/2$, and in (b) with respect to y at fixed $x = \pi/6$.

and the final time condition

$$\begin{aligned} u(x,y,T) &= x+y+\sin x \sin y \cos(2T), \\ u_t(x,y,T) &= -2\sin x \sin y \sin(2T). \end{aligned} \tag{40}$$

The data to be retrieved are given by

$$u(x,y,t) = x+y+\sin x \sin y \cos(2t),\ 0 \le t < T. \tag{41}$$

Fig. 4(a) indicates the errors of numerical solutions acquired from the BGPS for the case of T = 1 where the grid lengths $\Delta x = \Delta y = \pi/40$ and the time stepsize $\Delta t = 10^{-4}$. At the point $x = 5\pi/40$, the error is plotted with respect to y by a dashed line, and at the point $y = 19\pi/40$, the error is plotted with respect to x by a solid line. The latter one is smaller than the former one because the point $y = 19\pi/40$ is near the boundary.

When applied the BGPS to this experiment, we give a long temporal test of the BGPS with T = 4.6. Nevertheless, we can use the BGPS to retrieve the desired initial data x+y+sin$x$sin$y$, which is in the order of $O(1)$. The errors of numerical solutions calculated by the BGPS with $\Delta x = \Delta y = \pi/40$ and $\Delta t = 10^{-4}$ in the calculation are shown in Fig. 4(b), where at the point $x = 5\pi/40$, the error is plotted with respect to y by a dashed line, and at the point $y = 19\pi/40$, the error is plotted with respect to x by a solid line. For this very difficult problem, the BGPS proposed here is also good with a maximum error 5.09×10^{-3}.

In Fig. 5, we compare the numerical errors with T = 0.5 for two cases: one without the random noise and the other with the random noise in the level of s = 0.01. The exact solutions and numerical solutions are plotted in Figs. 6(a)-(c) sequentially. Even under the noise, the numerical solution illustrated in Fig. 6(c) is a good approximation to the exact initial data as shown in Fig. 6(a).

4.3 Example 3

Let us ponder a three-dimensional BWP:

$$u_{tt} = u_{xx} + u_{yy} + u_{zz},\ 0 < x < \pi,\ 0 < y < \pi,\ 0 < z < \pi,\ 0 < t < T, \tag{42}$$

with the boundary conditions

$$\begin{aligned} &u(0,y,z,t) = \exp(y+z+t),\ u(\pi,y,z,t) = \exp(\pi+y+z+t),\\ &u(x,0,z,t) = \exp(x+z+t),\ u(x,\pi,z,t) = \exp(\pi+x+z+t),\\ &u(x,y,0,t) = \exp(x+y+t),\ u(x,y,\pi,t) = \exp(\pi+x+y+t), \end{aligned} \tag{43}$$

and the final time condition

$$\begin{aligned} &u(x,y,z,T) = \exp(x+y+z+T),\\ &u_t(x,y,z,T) = \exp(x+y+z+T). \end{aligned} \tag{44}$$

The exact solution is given by

$$u(x,y,z,t) = \exp(x+y+z+t). \tag{45}$$

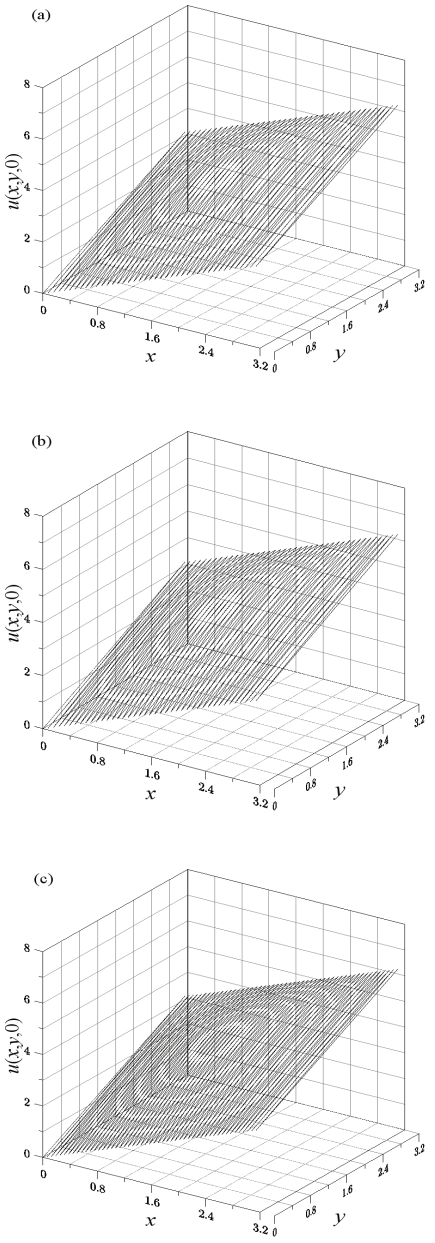

Figure 6: The exact solution for Example 2 of two-dimensional BWP with $T = 0.5$ are shown in (a), in (b) the BGPS solution without random noise effect, and in (c) the BGPS solution with random noise.

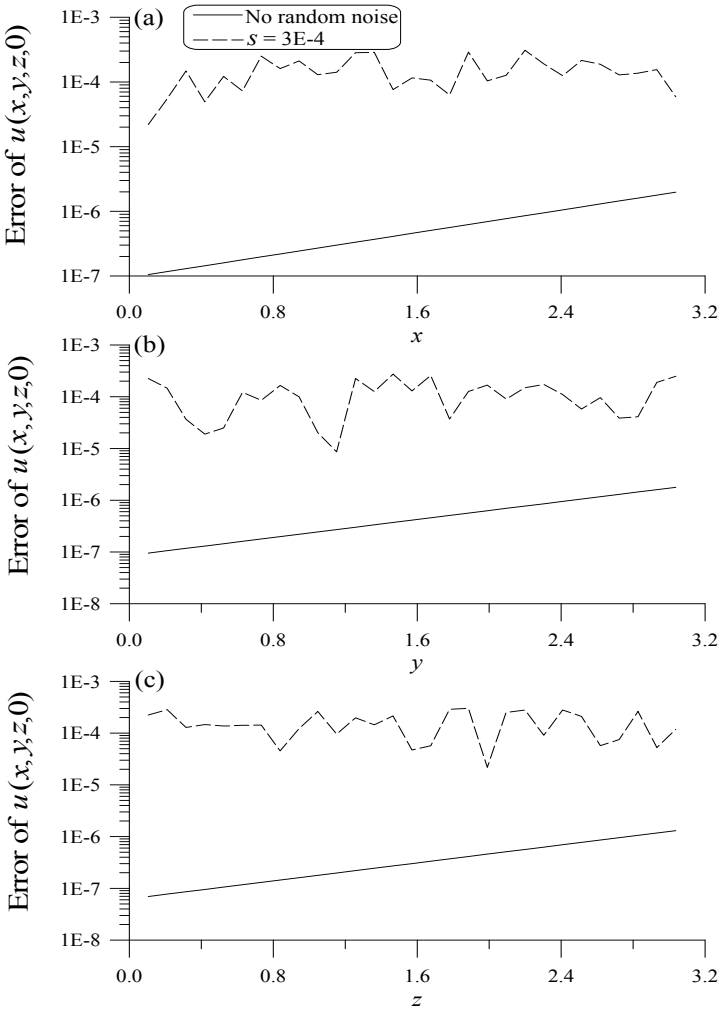

Figure 7: The numerical errors of BGPS solutions with and without random noise effect for Example 3 are plotted in (a) with respect to x at fixed $y = \pi/4$ and $z = \pi/3$, (b) with respect to y at fixed $x = \pi/5$ and $z = \pi/3$, and (a) with respect to z at fixed $x = \pi/5$ and $y = \pi/4$.

In Fig. 7, we compare the numerical errors with $T = 10$ for two cases: one without the random noise and the other with the random noise in the level of $s = 0.0003$. The exact solutions and numerical solutions are plotted in Figs. 8(a)-(c) sequentially. Even under the noise, the numerical solution displayed in Fig. 8(c) is a good

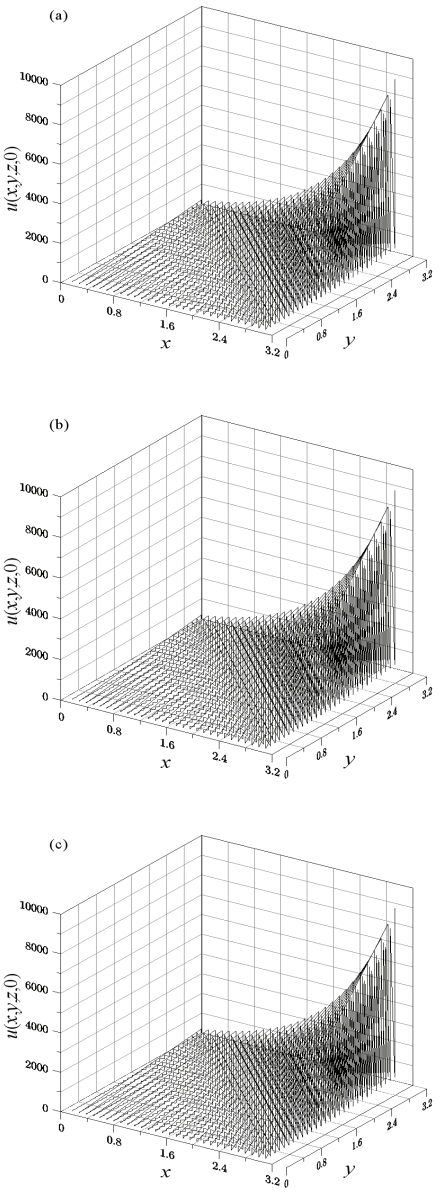

Figure 8: The exact solution for Example 3 of three-dimensional BWP with $T = 10$ are shown in (a), in (b) the BGPS solution without random noise effect, and in (c) the BGPS solution with random noise.

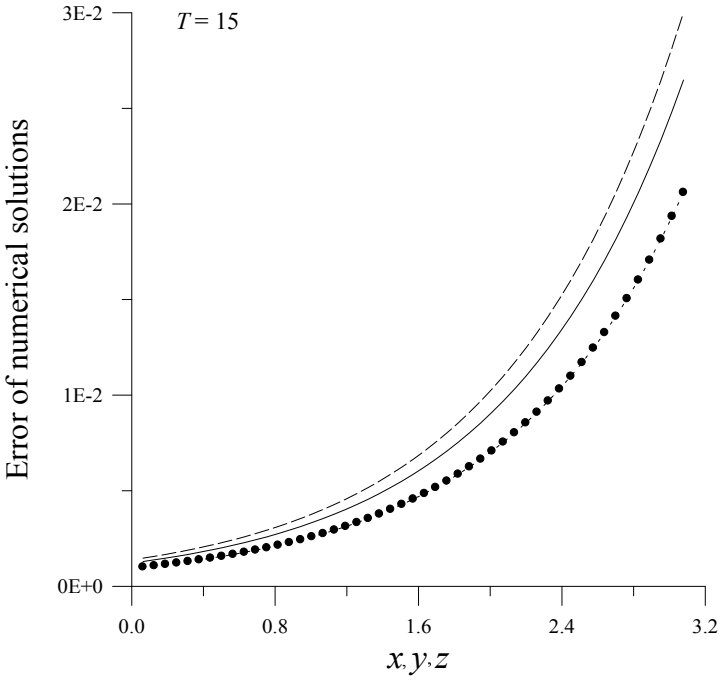

Figure 9: The errors of BGPS solutions for Example 3 with $T = 15$.

approximation to the exact initial data as displayed in Fig. 8(a).

To give a stringent test of the BGPS when applied the BGPS to this example, we let $T = 15$, and the final data are very large in the order of $O(10^{10})$. However, we can use the BGPS to retrieve the desired initial data $\exp(x+y+z)$, which are in the order of $O(10^5)$. In Fig. 9, we compare the numerical errors with $T = 15$, where the grid lengths are taken to be $\Delta x = \Delta y = \Delta z = \pi/50$ and the time stepsize is taken to be $\Delta t = 15$. At the point $x = \pi/5$ the error is plotted with respect to y and z by a dashed line, at the point $y = \pi/4$ the error is plotted with respect to x and z by a solid line, and at the point $z = \pi/3$ the error is plotted with respect to x and y by a dotted line. The latter one is smaller than the former two because the point $z = \pi/3$ is near the boundary. This example is a hard BWP problem to examine the numerical performance of novel numerical approaches. Nevertheless, to the authors' best knowledge, there has been no report that numerical schemes can calculate this ill-posed multi-dimensional BWP very well as our method.

5 Conclusions

These multi-dimensional BWPs have been calculated by the formulation with a semi-discretization of the spatial coordinate of backward wave equations together with the backward group preserving numerical integration algorithm. In this article, we are concerned about this numerical integration problem, in which the vital point is the creation of a past cone and a BGPS. Besides, we can construct a past cone, Lie algebra and Lie group delineation of the backward problems governed by differential equations. On the basis of those numerical experiments, we demonstrate that the BGPS is applicable to the multi-dimensional BWP, and even for the very severely ill-posed ones. The numerical errors of our scheme are in the order of $O(10^{-2})$–$O(10^{-8})$. Under specific grid spacing lengths and time step-sizes, the BGPS can produce an accurate result, and the implementation is simple. Furthermore, the efficiency of one-step BGPS is rooted in the closure property of the Lie group that we utilize it to establish the numerical approach for the multi-dimensional BWP.

Acknowledgement: The corresponding author would like to express his thanks to the National Science Council, ROC, for their financial supports under Grant Numbers, NSC 99-2218-E492-005.

References

Abdul-Latif, A. I.; Diaz, J. B. (1971): Dirichlet, Neumann, and mixed boundary value problems for the wave equation $u_{xx} - u_{yy} = 0$ for a rectangle. *Appl. Anal.*, vol. 1, pp. 1–12.

Ames, K. A.; Straughan, B. (1997): Non-standard and Improperly Posed Problems, Academic Press, New York.

Bourgin, D. G.; Duffin, R. (1939): The Dirichlet problem for the vibrating string equation. *Bull. Amer. Math. Soc.*, vol. 45, pp. 851–858.

Chabassier, J.; Joly, P. (2010): Energy preserving schemes for nonlinear Hamiltonian systems of wave equations application to the vibrating piano string. *Comput. Methods Appl. Mech. Engrg.*, vol. 199, pp. 2779–2795.

Czygan, O.; von Estorff, O. (2003): An analytical fundamental solution of the transient scalar wave equation for axisymmetric systems. *Comput. Methods Appl. Mech. Engrg.*, vol. 192, pp. 3657–3671.

Fox, D.; Pucci, C. (1958): The Dirichlet problem for the wave equation. *Ann. Mat. Pura Appl.*, vol. 46, pp. 155–182.

Gu, M. H.; Young, D. L.; Fan, C. M. (2009): The method of fundamental solution

for one-dimensional wave equations. *CMC: Computers, Materials & Continua*, vol. 11, pp. 185–208.

Lesnic, D. (2002): The decomposition method for forward and backward time-dependent problems. *J. Comp. Appl. Math.*, vol. 147, pp. 27–39.

Levine, H. A.; Vvessella, S. (1985): Stabilization and regularization for solutions of an ill-posed problem for the wave equation. *Math. Meth. Appl. Sci.*, vol. 7, pp. 202–209.

Liu, C.-S. (2001): Cone of non-linear dynamical system and group preserving schemes. *Int. J. of Non-Linear Mech.*, vol. 36, pp. 1047–1068.

Liu, C.-S. (2004): Group preserving scheme for backward heat conduction problems. *Int. J. Heat Mass Transfer*, vol. 47, pp. 2567–2576.

Liu, C.-S. (2006): An efficient backward group preserving scheme for the backward in time Burgers equation. *CMES: Computer Modeling in Engineering & Sciences*, vol. 12, pp. 55–65.

Liu, C.-S.; Chang, C.-W.; Chang, J.-R. (2006): Past cone dynamics and backward group preserving schemes for backward heat conduction problems. *CMES: Computer Modeling in Engineering & Sciences*, vol. 12, pp. 67–81.

Liu, C.-S.; Chang, C.-W.; Chang, J.-R. (2010): The backward group preserving scheme for 1D backward in time advection-dispersion equation. *Num. Meth. Partial Diff. Eq.*, vol. 26, pp. 61–80.

Yang, S. D. (2006): Shooting methods for numerical solutions of exact controllability problems constrained by linear and semilinear wave equations with local distributed controls. *Appl. Math. Comp.*, vol. 177, pp. 128–148.

Young, D. L.; Gu, M. H.; Fan, C. M. (2009): The time-marching method of fundamental solutions for wave equations. *Eng. Anal. Bound. Elem.*, vol. 33, pp. 1411–1425.

Zhou, W. J.; Ichchou, M. N. (2010): Wave propagation in mechanical waveguide with curved members using wave finite element solution. *Comput. Methods Appl. Mech. Engrg.*, vol. 199, pp. 2099–2109.